Probabilistic seismic assessment of RC box-girder bridges retrofitted with FRP and steel jacketing

Ali Naseri[1a], Alireza Mirzagoltabar Roshan[*2], Hossein Pahlavan[3b]
and Gholamreza Ghodrati Amiri[4c]

[1]Department of Structural Engineering, Babol Noshirvani University of Technology, Iran
[2]Department of Structural Engineering, Faculty of Civil Engineering,
Babol Noshirvani University of Technology, Iran
[3]Department of Earthquake Engineering, Shahrood University of Technology, Iran
[4]Center of Excellence for Fundamental Studies in Structural Engineering, School of Civil Engineering,
Iran University of Science and Technology, Iran

Abstract. Due to susceptibility of bridges in the past earthquakes, vulnerability assessment and strengthening of bridges has gained a particular significance. The objective of the present study is to employ an analytical method for the development of fragility curves, as well as to investigate the effect of strengthening on the RC box-girder bridges. Since fragility curves are used for pre- and post-earthquake planning, this paper has attempted to adopt the most reliable modeling assumptions in order to increase the reliability. Furthermore, to acknowledge the interaction of soil, abutment and pile, the effect of different strengthening methods, such as using steel jacketing and FRP layers, the effect of increase in the bridge pier diameter, and the effect of vertical component of earthquake on the vulnerability of bridges in this study, a three-span RC box-girder bridge was modeled in 9 different cases. Nonlinear dynamic analyses were carried out on the studied bridges subjected to 100 ground motion records via OpenSEES platform. Therefore, the fragility curves were plotted and compared in the four damage states. The results revealed that once the interaction of soil and abutment and the vertical component of the earthquake are accounted for in the calculations, the median fragility is reduced, implying that the bridge becomes more vulnerable. It was also confirmed that steel jackets and FRP layers are suitable methods for pier strengthening which reduces the vulnerability of the bridge.

Keywords: vulnerability assessment; steel jacketing; FRP layers; vertical component of earthquake; RC box-girder bridge

1. Introduction

Earthquake is one the most important natural phenomena that may sometimes cause economic loss in structures and human casualties in many countries. The road bridges, considered as the main and vital structures constructed on the essential municipal artery, can deliver adverse consequences

---

*Corresponding author, Associate Professor, E-mail: ar-goltabar@nit.ac.ir
[a]Ph.D. Candidate, E-mail: Alinaseri@stu.nit.ac.ir
[b]Assisstant Professor, E-mail: Pahlavan@Shahroodut.ac.ir
[c]Professor, E-mail: Ghodrati@iust.ac.ir

during the seismic events (Raheem 2018). Undoubtedly, collapse of a bridge may risk the pedestrians and vehicles in the vicinity with severe dangers, thus necessitating the rehabilitation in the aftermath of an earthquake.

Several studies have so far been carried out in the development of seismic fragility curves of both existing and strengthened bridges (Nielson 2005, Padgett 2007, Falamarz-Sheikhabadi and Zerva 2017). According to these studies, columns are the most vulnerable locations for damage in bridges. In the process of vulnerability evaluation, the difference between design assumptions and the existing state parameters may significantly alter the estimation of capacity and demand in bridges.

Pedgett and DesRoches (2008), presented an analytical approach for developing fragility curves. They investigated a simply-supported concrete box girder bridge strengthened with five different methods, i.e., steel jackets, seismic isolators, stayed cable, shear keys and seat extender. Results demonstrated that the most effective strengthening method in reducing damage probability is a function of the damage state.

Alim and Zisan (2013) studied a class of bridges strengthened with FRP. The fragility curves were then presented for both strengthened and unstrengthened cases. It was concluded that the strengthened case was less damaged.

Pahlavan *et al*. (2015) evaluated the seismic vulnerability of four-span RC curved bridges with regular column height by means of probabilistic approach. Developing fragility curves, they carried out different probabilistic methods of bridge retrofitting. The result revealed the significant influence of various retrofitting methods on the seismic performance of bridge.

Few investigations have already been conducted on the vulnerability assessment and fragility curves regarding the vertical component of the earthquake (Pahlavan 2015). Such studies have only examined the performance of bridges subjected to a limited number of records thru a deterministic evaluation of seismic damage to bridges.

In this paper, the probabilistic evaluation of bridge damage is investigated by making use of fragility curves, where identifying such an issue is of high practical importance in subsequent decisions for rehabilitation and strengthening purposes. In addition, two types of strengthening with steel jackets and FRP layers are applied on the bridge piers and the results are compared with the unstrengthened specimens.

2. Seismic strengthening

Most column damages can be attributed to the insufficient detailing that limits the inelastic ductility of the column. For concrete piers, this may result in bending, shear, splice or anchorage fracture or a combination of these mechanisms. An example of the bridge column failure is shown in Fig. 1.

The results of articles indicate that strengthening with FRP can be effective in recovering the original strength of bridge girders with damaged end regions (Shaw and Andrawes 2017).

Due to the high importance of piers, the strengthening strategy of the present paper is focused on this component with an example shown in Fig. 2.

3. Verification

This section aims at determining the accuracy of nonlinear modeling methods in the estimation

Fig. 1 Example of the bridge column failure

Fig. 2 Strengthening of the bridge piers with FRP layers
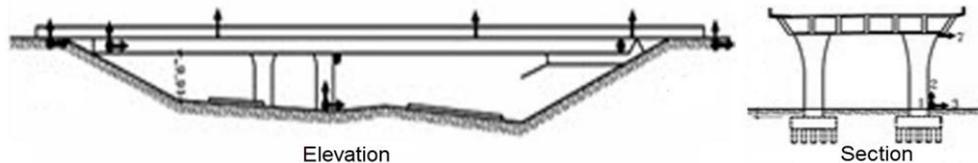
Fig. 3 The overall view of "Painter Bridge" (Zhang and Makris 2002)

of dynamic response of bridges. Thereby, the actual results of the "Painter Bridge" are used as benchmarks. This bridge is located at Riodell 101 Ave., California State and was constructed in 1976 in a skew form with box girders whose concrete was cast integrated with columns and abutments. The bridge is 15.85 m wide and consists of two spans of 44.5 m and 35 m long with skew angle of 39 degrees and circular column sections of varied diameter from 1.5 m at the foundation to 2.7 m at the connection to deck. The piers are about 7.32 m high, each supported by 20 concrete friction piles. The east and west abutments are supported by 14 and 16 piles, respectively. The east abutment has integrated concrete with its foundation while the west one sits on the foundation through an elastomeric support so as to allow thermal deformations. A shear key, with the same width as abutment, is provided on pile cap with a distance of 2.5 cm from the abutment wall in order to prevent inadmissible longitudinal deformations of the bridge.

Furthermore, other shear keys are used on pile caps to control transverse deformations of the bridge on the northern and southern sides of the abutment.

This bridge has been equipped with ground motion recording instruments since 1997. The overall view of the bridge is depicted in Fig. 3 (Zhang and Makris 2002).

Due to the integrity of deck and abutments, these members were modeled as rigid vertical elements. Soil behavior conformed to hyperbolic model proposed by Shamsabadi and Yan (2008), based on experiments conducted on typical soils. Mean initial stiffness was set equal to 37 *kN/mm* for active soil pressure, and the failure displacement was defined on the hyperbolic curve of Sahmsabadi, corresponding to 10% of the abutment height.

Comparison of the results from analytical model with those of actual data recorded via sensors in the vicinity of abutments and top of the column under the 1992 Petrolia earthquake is presented in Figs. 4 and 5. By comparing the results of the analytical model with those recorded by sensors, it is seen that the maximum difference between the two in the longitudinal and transverse directions is approximately 13 and 7%, respectively. These figures confirm the reasonable accuracy of the analytical model.
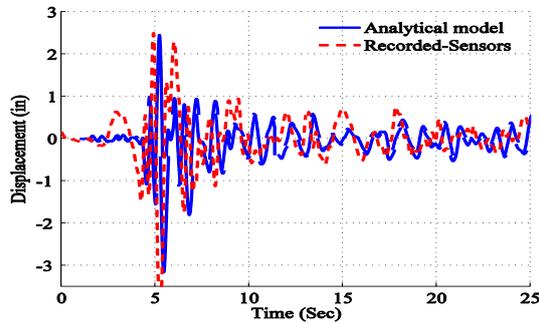
Fig. 4 Comparison of analytical model results with the actual data in transverse direction
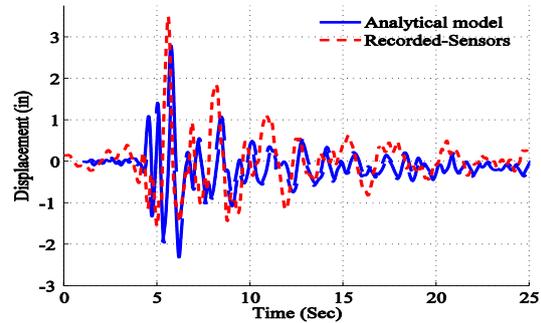
Fig. 5 Comparison of analytical model results with the actual data in longitudinal direction

Table 1 Modeling specifications

Model Number	Column diameter(m)	
1	1	Without the effect of soil interaction and abutment
2	1.5	Without the effect of soil interaction and abutment
3	1	With the effect of soil interaction and abutment
4	1.5	With the effect of soil interaction and abutment
5	1	Strengthened with FRP layers with the effect of soil interaction and abutment
6	1	Strengthened with steel jackets with the effect of soil interaction and abutment
7	1	With the effect of soil interaction and abutment and vertical component of earthquake
8	1	Strengthened with FRP layers with the effect of soil interaction and abutment and vertical component of earthquake
9	1	Strengthened with steel jackets with the effect of soil interaction and abutment and vertical component of earthquake

4. Modeling the members of studied bridge

In order to gain more precise control of bridge behavior in the course of the earthquake, the *OpenSEES* (McKenna *et al*. 2009) finite element program is used in the present study. In addition, a horizontally RC box-girder highway bridge located in the north of Iran is investigated. The bridge comprises 3 spans of 24.5 m (total of 73.5 meters), where a girder deck of 11.9 m width is supported by two piers each encompassing three circular concrete columns of 9.52 m.
Since two-dimensional (2D) analysis of the bridge is unable to model the interaction of different bridge components, thus leading to considerable errors in the response calculation, a 3D model is used herein.

A total of nine models are used in this paper with the characteristics given in Table 1. In the first two models, the interaction between abutment and soil beneath the column is ignored, and thus the column base is considered to be fixed. However, these effects have been considered in models 3 and 4. Models 5 and 6 are similar to model 3, though strengthened respectively with FRP layers and steel jackets. In model 7, 8 and 9, the effect of vertical component of earthquake on the strengthened and unstrengthened bridges is considered. In the end, the effects of each of the parameters are included in the vulnerability of the bridges.
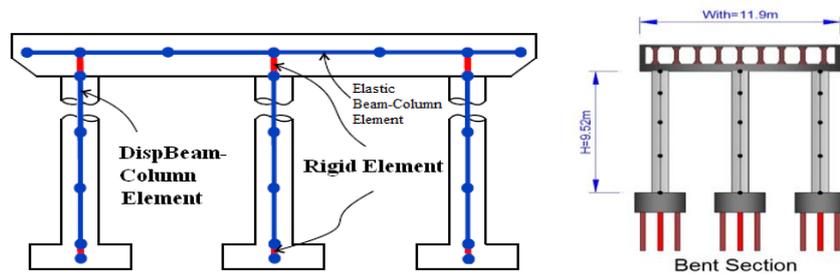
Fig. 6 Modeling of the deck, columns, and column caps in *OpenSEES* platform

4.1 Concrete and steel materials

Both confined and unconfined tensile strengths of the utilized concrete were considered in the bridge modeling. It is worth noting that a single stress-strain model should be used in defining both concrete types in the estimation of capacity and ductility of concrete members. The prevailing Mander's model was used for stress-strain relation of confined concrete, featuring cyclic loading and including strain rate effects (Mandar *et al*. 1988). For the definition of concrete and steel materials, the concrete07 and steel 02 were assigned respectively from the OpenSEES library.

The most ideal condition in the mass distribution amongst bridge elements is to act based upon their lengths. In the model used herein, transitional and rotational masses were assigned to sufficient number of nodes in different directions.

4.2 Modeling of bridge deck and piers

The modeling of bridge deck has a considerable effect on the dynamic response and behavior of that bridge. In this study, bridge deck was modeled linearly since is not expected to enter the nonlinear region and the thus Elastic Beam Column Element was assigned to it (Nielson 2005, Padgett 2007). Such elements were also used for modeling the column caps.

The bridge piers are sub-structural components for supporting deck in both horizontal and vertical directions. Hence, for the modeling of columns with inelastic elements, the total length of column was assumed to be susceptible to the formation of plastic hinge and then DispBeamColumn Elements were used in *OpenSEES*, as shown in Fig. 6.

4.3 Bridge abutment

Among the various procedures in modeling abutments, the model proposed by Aviram *et al*. (2008) was practiced in which a set of nonlinear springs was considered for simulating the abutment behavior. The modeling of pile and soil should be adopted as it follows.

4.3.1 Soil

Hyperbolic gap materials proposed by the latest studies carried out by Shamsabadi and Yan (2008) were used to model the soil at the back of the abutment (Fig. 7). These researchers applied two numerical models (spiral semi-hyperbolic logarithmic model and finite element model) to establish a hyperbolic force- displacement relationship by using experimental results conducted on actual abutments. Such relation is expressed in Eq. (1)

Table 2 Soil characteristics (Shamsabadi and Yan 2008)

Soil type	a	b	c	n
non-cohesive	410.6	1.867	0.05	1.56
cohesive	249.1	0.8405	0.1	1.05

$$F(y) = \frac{ay}{H+by} \times H^n, (\frac{y}{H} < C) \tag{1}$$

Where F is the lateral force in unit width of the wall for the lateral displacement of y, H denotes abutment height, and a, b, c and n are constants with different values for non-cohesive and cohesive soils as given in Table 2.

4.3.2 Pile

Choi tri-linear model was used to simulate the piles. Piles and soil act as two parallel springs in the longitudinal direction for the active case and hence their forces are summed up in the force-displacement diagram at equal displacements. On the other hand, only the piles act in transverse direction, as well as the longitudinal direction for the passive case (Pahlavan 2015), the tri-linear model is illustrated in Fig. 7, and the relation is given in Eq. (2).

$$
\begin{aligned}
K_{eff} &= 7\frac{KN}{mm} \\
K_1 &= \frac{7}{3}K_{eff} \\
K_2 &= 0.428K_{eff} \\
\Delta_1 &= 7.62mm \\
\Delta_2 &= 25.4mm
\end{aligned}
\tag{2}
$$

in which K_{eff} is the strength of one pile, K_1 and K_2 are existing parameters in the relation, and Δ_1 and Δ_2 are allowable displacements. Once the bearing capacity of the piles are determined, piles are modeled via zero-length elements

4.4 Elastomeric bearing pads

Elastomeric bearing pads are typically used as supports in concrete bridges that transfer the horizontal loads through friction and their behavior depends very much on the initial stiffness. In the bridge under study, elastomeric pads were used at the location of caps and abutments with the same number of the webs of deck section (one pad was used beneath each web).

By increasing friction, stiffness of the bearing pad tends toward zero. Thus, the response of these members can be modeled by elastic-perfectly plastic materials as shown in Fig. 7 (Pahlavan 2015). Steel01 material was used in *OpenSEES* to model such behavior. F_y is the ultimate strength of elastomer, and K_{pad} is the initial stiffness of its material which is determined from Eq. (3) where G is the shear modulus, A the section area, and h the pad thickness

$$K_{pad} = \frac{GA}{h} \tag{3}$$
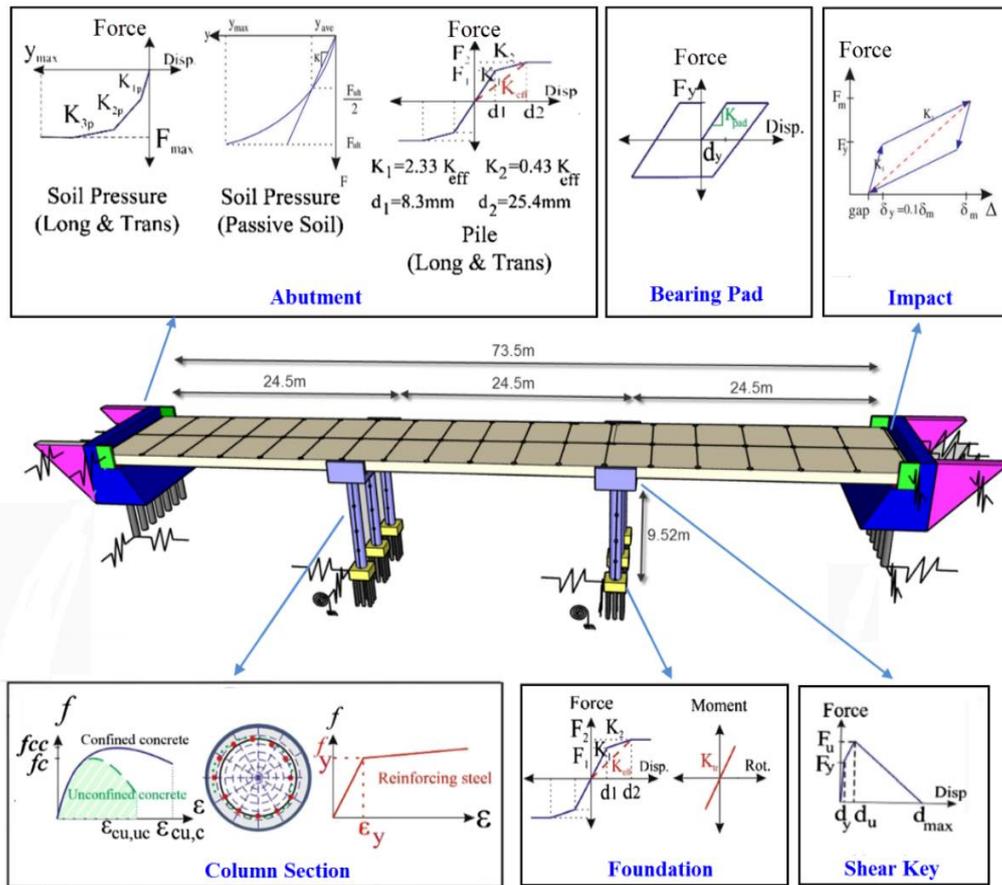
Fig. 7 Analytical model of the bridge and components with nonlinear behaviors

The yielding force, F_y, is the product of vertical load applied to the support and the coefficient of friction of pad. Scharge (1981) presented Eq. (4) for the coefficient of friction in concrete surfaces, based on the empirical observations, in which σ_m is the normal stress applied to pad in MPa.

$$\mu = 0.05 + \frac{0.4}{\sigma_m} \tag{4}$$

Zero-length elements were also used for elastomeric pads in both longitudinal and transverse directions. It is indeed assumed that the supports act in both longitudinal and transverse directions.

4.5 Shear keys

Shear keys are often used in bridges with short- to medium-span lengths in order to provide a lateral support for the bridge superstructure. These elements do not carry gravity loads, but transfer the reaction from superstructure to abutment and column caps during the earthquake. The loads are subsequently transferred to ground through piles and walls adjacent to abutments, as well as the columns through shear.

According to field tests conducted at Caltrans and San Diego University by Megally *et al.* (2001),

shear keys have nonlinear behavior (Fig. 7). In this study, the behavior of shear key was modeled as shown in Fig. 7. Moreover, the design of shear key was based on 75% of shear capacity of the total columns present in the abutments (Caltrans 2010, 2012).

Hysteretic materials were used in *OpenSEES* to describe the shear key behavior. The parameters related to such materials were defined such that the function of keys is identical to fuses, that is, they do not sustain strength after the failure. Again, zero-length elements were applied in just transverse direction.

4.6 Impact element

Collision of bridge components (deck and abutment wall) are among cases proven to be highly effective on the seismic response of bridges. Therefore, their inclusion is necessary in the analytical modeling. One of the typical methods to do so is to use impact elements which are activated only when the gap is closed. The analytical model of such elements is demonstrated in Fig. 7. Ramanatan (2012) has presented the following values of impact element parameters for a width of 1 *m* which are modified based on the distance between nodes in abutment (Eq. (5)).

$$
\begin{aligned}
K_1 &= 587.3466 \ \text{KN/mm/m} \\
K_2 &= 202.0954 = 4 \ \text{KN/mm/m} \\
\delta_m &= 25.4 \ \text{mm} \\
\delta_y &= 0.1 \times \delta_m = 2.54 \ \text{mm}
\end{aligned}
\tag{5}
$$

4.7 Modeling FRP layers and steel jacket

For the modeling of the effect of FRP layers and steel jacket, it is adequate to use the relationships proposed for concrete confinement. Eqs. (6) and (7) were used to calculate the confinement with FRP (Wu and Wang 2009), and Eqs. (8) and (9) were used for steel jacket (Sakino 1994).

$$
\frac{f_{cc}'}{f_{c0}'} = 1 + 2.2 \left(\frac{f_l}{f_{c0}'} \right)^{0.94}
\tag{6}
$$

$$
f_l = \frac{2 f_{frp} t}{d}
\tag{7}
$$

where f_{frp} is the tensile strength of FRP in longitudinal direction of strap, t is the total thickness of layer, and d is the diameter of confined concrete core.

$$
K = \frac{f_{cc}'}{f_c'} = 1 + 11.5 \frac{\rho_t f_{yt}}{f_c'} \left(\frac{t}{B - 2t} \right)
\tag{8}
$$

$$
\rho_t = \left(\frac{B}{B - 2t} \right)^2 - 1
\tag{9}
$$

In Eqs. (8) and (9), f_c', ρ_t, f_{yt}, t and B are respectively the concrete cylindrical strength (in MPa), density, steel yield stress, thickness, and diameter of steel jacket.

The modeling of various bridge elements in *OpenSEES* platform is summarized in Table 3. Likewise, the random variables of different bridge members are presented in Table 4.

Table 3 Behavior of different bridge components and modeling in *OpenSEES*

Bridge component or material	Modeled element type and behavior	References
Deck	Elastic beam-column element with calculated section properties	Nielson (2005)
Column	Nonlinear beam-column element with fiber section	Nielson (2005)
Elastomeric bearings	Elastic-perfectly-plastic behavior with steel 01 material applied to zero length element	Nielson (2005)
Impact	Bilinear behavior applied to zero length element	Ramanatan (2012), Muthukumar and DesRoches (2006).
Piles	Uniaxial material hysteretic with trilinear behavior	Choi (2002)
Abutment	Hyperbolic gap material with parabolic soil behavior which applied to zero length element	Shamsabadi *et al.* (2010), Choi (2002)
Shear key	Uniaxial hysteretic behavior applied to zero length element	Megally *et al.* (2001)
Concrete	Concrete 07 material with monotonic stress-strain characteristic	Chang and Mander (1994)
Reinforcing steel bars	Steel 02 material with isotropic strain hardening behavior	Menegotto and Pinto (1973)

Table 4 Random variables and distributions available in different bridge components

Modeling parameter	Probability distribution	Distribution parameter			References
		1	2	Units	
Steel yield strength	Lognormal	$\lambda=29$	$\zeta=0.08$	MPa	Ellingwood and Hwang (1985)
Concrete unconfined strength	Normal	$\mu=34.5$	$\sigma=4.3$	MPa	Choi (2002)
Elastomeric bearing shear modulus	Uniform	$l=551$	$u=1.723$	MPa	Ramanathan (2012)
Coefficient of friction MF|t2fn1	Lognormal	$\lambda=0$	$\zeta=0.1$	----	Mander *et al.* (1996), Dutta (1999)
Piles rotational stiffness	------	0	0	----	CALTRANS (2007)
Piles translational stiffness	Lognormal	$\lambda=7.06$	$\zeta=0.3$	kN/mm/pile	CALTRANS (2007)
Abutment passive initial stiffness [a]	Uniform	$l=14.5$	$u=29$	kN/mm/m	Shamsabadi *et al.* (2010)
Damping	Normal	$\mu=0.045$	$\sigma=0.0125$	----	Fang *et al.* (1999), Bavirisetty *et al.* (2000)
Abutment gap	Uniform	$l=38.1$	$u=152$	mm	Based upon inventory review
Mass	Uniform	$l=1.1$	$u=1.4$	----	Ramanathan (2012)
Loading direction	Uniform	$l=0$	$u=2\pi$	rad	Ramanathan (2012)
Percentage of longitudinal column bars	Uniform	1%	3.7%	----	Ramanathan (2012)
Gap between deck and Abutment	Uniform	0	10	cm	Ramanathan (2012)
Gap between deck and shear key in transverse direction	Uniform	0	4	cm	Ramanathan (2012)

[a] Variables are per unit width of the abutment backwall.

First mode

Second mode

Third mode
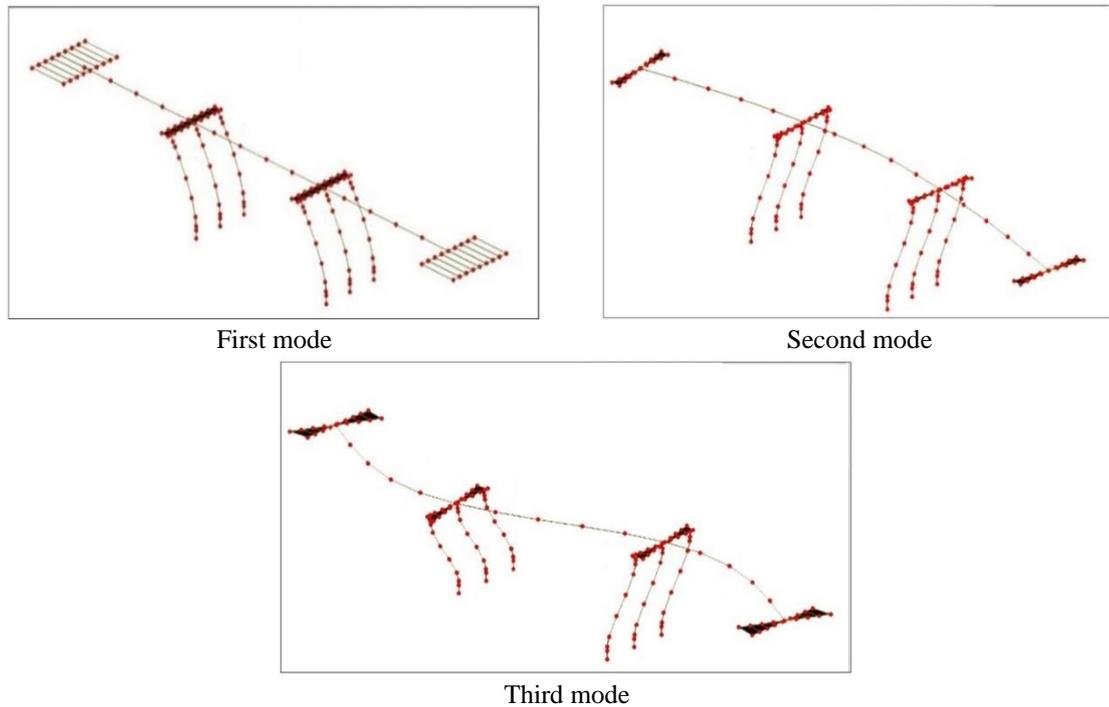
Fig. 8 The first three modes of the bridge

4.8 Mode shapes

Mode shapes of the first three modes of the bridge under study are shown in Fig. 8. It is worth noting that the dominant mode (the first) is in the longitudinal direction, the second mode is in the transverse direction and the third mode is the torsion about the vertical axis.

5. Selection of earthquake records

Nonlinear dynamical analysis is one of the most accurate analyzes available, which has been used for many bridges (Baloevic *et al*. 2016).

One of the most important factors in the dynamic time-history analysis is to determine the records applied to structure, since the obtained results may be strongly dependent on the record.

Baker *et al*. (2011) at the civil engineering department of Stanford University and the Pacific Earthquake Engineering Research Center (PEER) offered a set of earthquake records for vulnerability evaluation of structures. A total of 100 records of these set were used in the present investigation.

These records were used by many researchers to explore the vulnerability of bridges (Padgett and DesRoches 2008, Pahlavan *et al*. 2015). This set of earthquake records embraces 40 far-fault and 60 near-fault records.

In this study, the nonlinear dynamic analysis was carried out by using Newmark integration theme presented in *OpenSEES* platform. Energy absorption in the structural elements is

Table 5 Limit-state capacities for various articles

	Slight		Moderate		Extensive		Complete		Bridge type
	S_c	β_c	S_c	β_c	S_c	β_c	S_c	β_c	
Abbasi *et al.* (2015), Pahlavan *et al.* (2015)	1	0.35	2	0.35	3.5	0.35	5	0.35	Multi-span multiframe concrete box-girder bridge
jeon *et al.* (2015)	0.5	0.25	1	0.25	2	0.46	2.5	0.46	Typical older two-span single frame concrete box-girder bridge
Jeon *et al.* (2016)	1	0.35	2	0.35	3.5	0.35	5	0.35	Multiframe RC box-girder bridges, multiple single-column bent
Siqueira *et al.* 2014	0.5	0.25	0.7	0.25	1.1	0.46	3	0.46	Multispan Concrete-girder bridges
Ramanathan *et al.* (2012) (non seismic)	1	0.25	1.58	0.25	3.22	0.47	4.18	0.47	Multispan continuous concrete girder / Multispan simply supported concrete girder
Ramanathan *et al.* (2012) (seismic)	1	0.25	5.11	0.25	7.5	0.47	9	0.47	Multispan continuous concrete girder / Multispan simply supported concrete girder
HAZUS-MH	0.91	0.6	0.91	0.6	1.05	0.6	1.38	0.6	Model HWB23, Continuous concrete, Seismic design

accomplished by Rayleigh damping and a 5% damping is assumed in the modeling of bridge.

Since the direction of applied earthquake with maximum stress in a particular member can't be determined before the analysis of complicated 3D structures such as bridges, the accelerations of dynamic analysis should be considered in various directions (Aviram *et al.* 2008).

6. Fragility analysis of bridges

For definition and classification of seismic damage in bridge structures, it is necessary to understand the different cases of seismic damages in order to determine the measure of damage and fragility matrices. Many researchers, such as Tondini and Stojadinovic (2012) considered the piers as the main parameters for evaluating bridge damage. Since the strength and stability of a bridge is strongly related to its pier strength, and the damage to the piers can endanger the safety and serviceability of the bridge, considering this component as the main parameter is logical.

β_c and S_c vary depending on the type of bridge and numerous researchers have considered different values for them, as shown in Table 5. In this study and for evaluating the vulnerability of bridge piers, the damage index proposed by Abbasi *et al.* (2015) and Pahlavan *et al.* (2015) is used due to its consistence with the models used here.

Since Abbasi *et al.* (2015) and Pahlavan *et al.* (2015) studied built multi-span multi-frame concrete box girder bridges and regarding the fact that the bridge studied here was also of this type and that the support and deck connections were the same, the damage indexes of these studies were used to evaluate the vulnerability of the bridge in this work.

The degree of damage can be assessed via a probabilistic model, once it is possible to determine the relation between an earthquake and the corresponding damage (Shinozuka *et al.* 2000).

The fragility curves determine the probability of exceeding a certain damage state, which can be calculated and plotted using the structural demand and capacity, each of which is expressed in terms of median and dispersion. The median and dispersion of demand can be achieved based on the
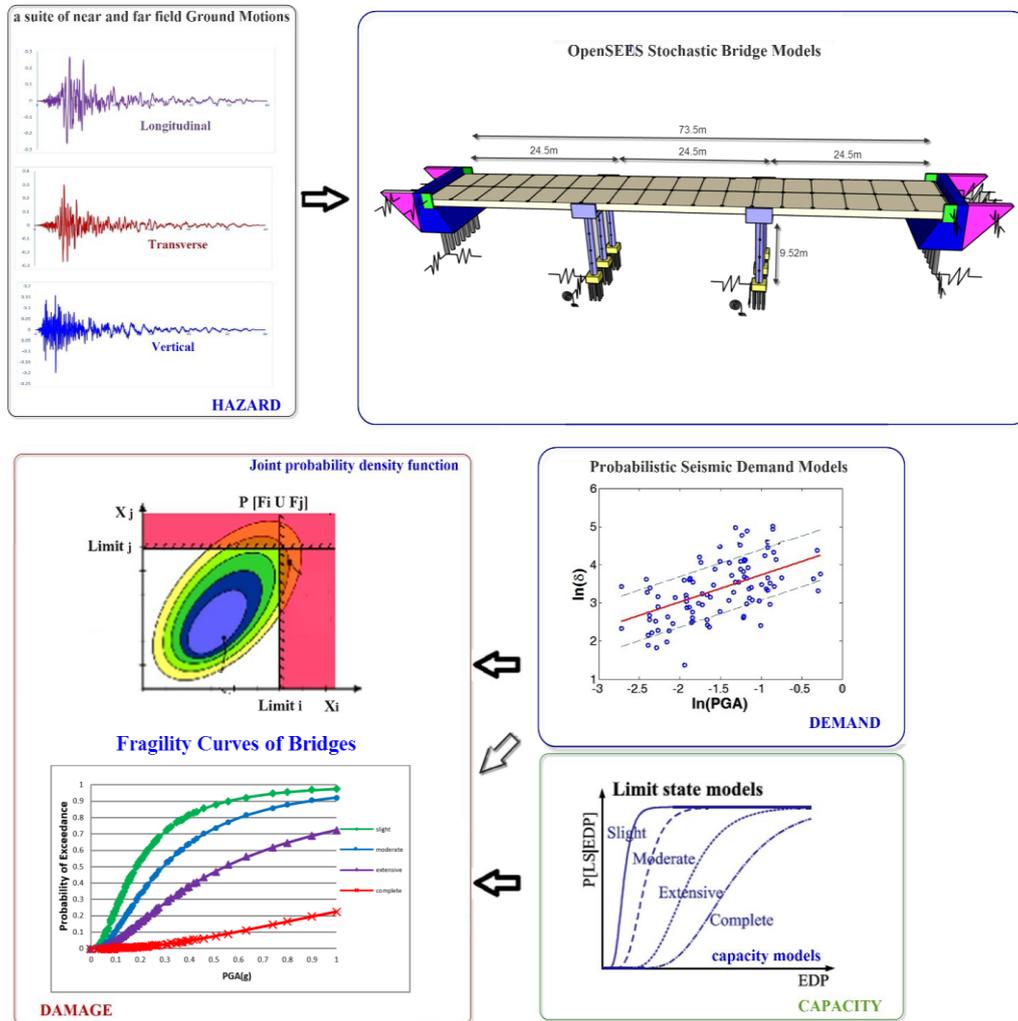
Fig. 9 Schematic of the probabilistic seismic assessment framework

regression on the set of recorded demands for a member. The median and dispersion of the capacity are attained on the basis of laboratory studies and observations from past earthquakes for different members.

These curves can be shown as a lognormal distribution function (Eq. (10)); in which P_f denotes the probability of exceeding a particular damage state, S_d and S_c are respectively the median value of seismic demand and median value of capacity.

$$P_f = P\left[\frac{S_d}{S_c} \geq 1\right]$$

(10)

If the demand and capacity are specified by logarithmic distributions, the probability of exceeding a particular damage state would have logarithmic distribution which can be estimated as follows (Eq. (11)).

$$P_f = \Phi \left[\frac{\ln\left(\dfrac{S_d}{S_c} \right)}{\sqrt{\beta_d^2 + \beta_c^2}} \right] \tag{11}$$

where β_d and β_c are respectively the dispersions of demand and capacity, and $\Phi[]$ is lognormal cumulative probability density function (*HAZUS-MH*). Seismic demand can be measured as follows (Eq. (12)) (Abbasi *et al.* 2015, Roshan *et al.* 2018, Naseri *et al.* 2017, Pahlavan *et al.* 2018, Shamekhi amiri *et al.* 2019).

$$\ln(S_d) = a \times \ln(IM) + b \tag{12}$$

in which *a* and *b* are coefficients obtained through the regression analysis, and IM is the intensity measure which was considered to be PGA in this study.

Fig. 9 shows a schematic of the aforementioned fragility framework.

9. Results and discussion

Fragility curves for models 1 to 9, introduced in Table 1, are compared to each other in Figs. 10-
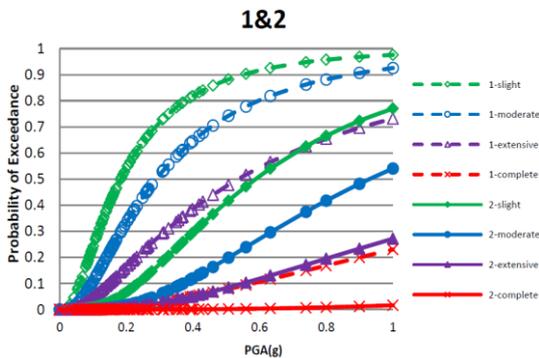
Fig. 10 Comparison fragility curves generated for model 1 and 2
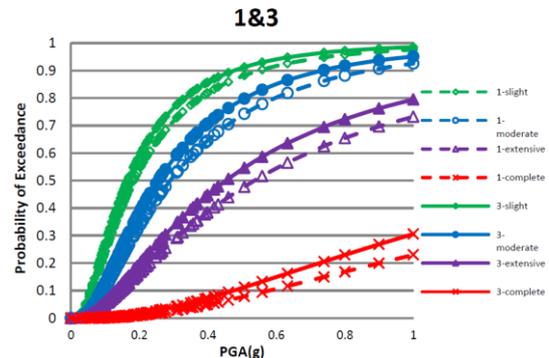
Fig. 11 Comparison fragility curves generated for model 1 and 3
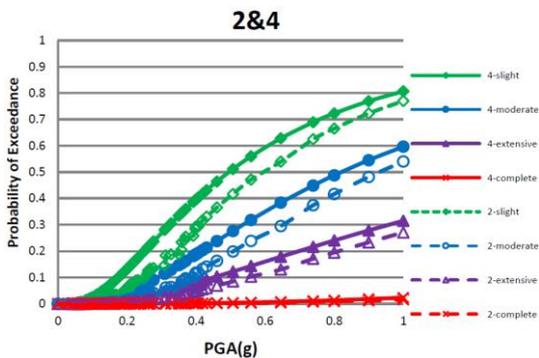
Fig. 12 Comparison fragility curves generated for model 2 and 4
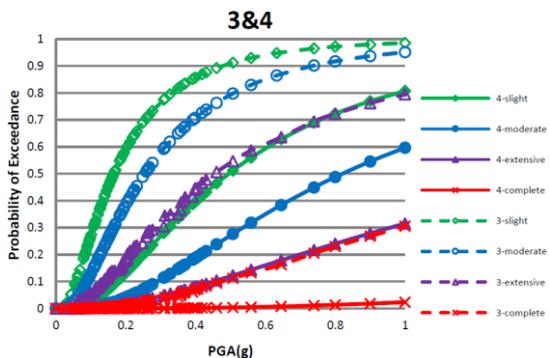
Fig. 13 Comparison fragility curves generated for model 3 and 4
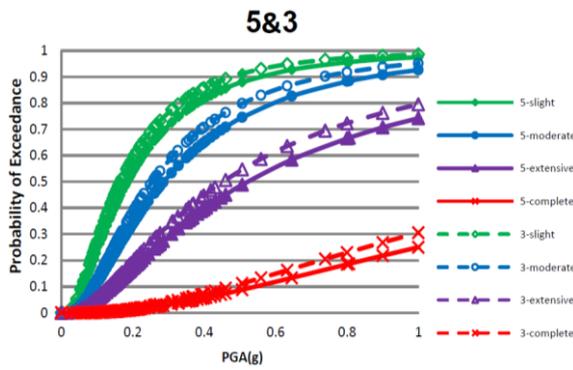
Fig. 14 Comparison Fragility curves generated for model 3 and 5
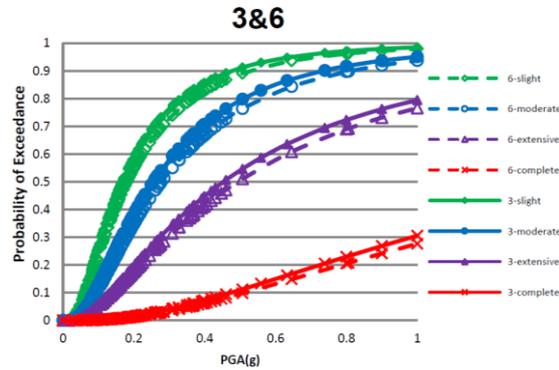
Fig. 15 Comparison Fragility curves generated for model 3 and 6
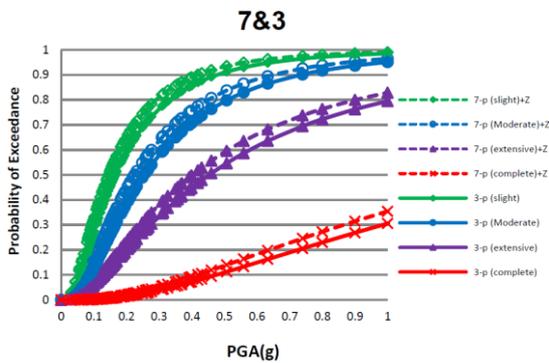
Fig. 16 Comparison Fragility curves generated for model 3 and 7
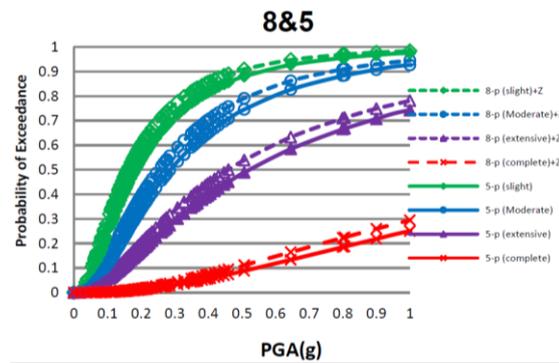
Fig. 17 Comparison Fragility curves generated for model 5 and 8
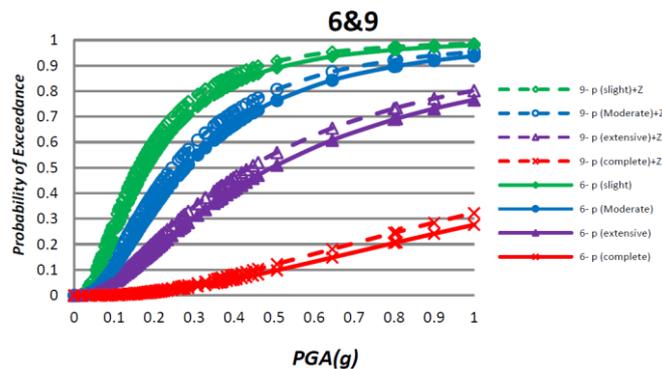
Fig. 18 Comparison Fragility curves generated for model 6 and 9

18 for the 4 damage states of slight, moderate, extensive and complete. In addition, median fragility, in which PGA corresponds to 50% of failure, is a good index for comparing fragilities with the values reported in Table 6.

It is noted that with increase in the median fragility, vulnerability of the bridge is reduced. By comparing the median values of fragility in 9 different states, it can be observed in Fig. 19 that, with

Table 6 Median Fragility for nine bridges at four damage states

Model NO	Slight		Moderate		Extensive		Complete	
	S_c	β_{sd}	S_c	β_{sd}	S_c	β_{sd}	S_c	β_{sd}
1	0.183	0.578	0.290	0.578	0.537	0.578	2.103	0.578
2	0.590	0.465	0.931	0.465	1.719	0.465	6.713	0.465
3	0.166	0.597	0.254	0.597	0.453	0.597	1.632	0.597
4	0.495	0.479	0.821	0.479	1.686	0.479	6.296	0.479
5	0.184	0.602	0.287	0.602	0.523	0.602	1.965	0.602
6	0.181	0.605	0.278	0.605	0.495	0.605	1.779	0.605
7	0.149	0.60	0.231	0.60	0.418	0.60	1.520	0.60
8	0.160	0.61	0.252	0.61	0.460	0.61	1.770	0.61
9	0.158	0.608	0.245	0.608	0.446	0.608	1.570	0.608
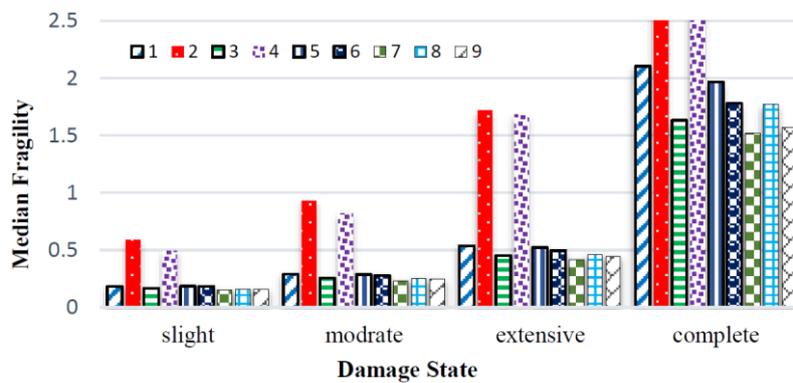
Fig. 19 Comparison of the impact of abutment and foundation, vertical earthquake component and Retrofitting method on the median values of fragility

increasing cross-sectional diameter of bridge piers from 1 m to 1.5 m in models 2 and 4, the bridge median fragility is escalated more than 3 folds compared to models 1 and 3.This indicates that the potential vulnerability of the bridge is sharply reduced by increasing the diameter of the column section.

In addition, by comparing models 1 vs. 3 and models 2 vs. 4, it can be concluded that considering the effect of abutment and foundation increases the probability of a bridge vulnerability, so that the median fragility is reduced by about 12% on average (Table 7).

By comparing each pair of the models 3 vs. 7, 5 vs. 8, and 6 vs. 9, it can be inferred that the effect of the vertical component of the earthquake on bridges causes an average of 10.6% reduction in the median fragility of the bridges (Table 7).

By comparing models 3 vs. 5 and models 7 vs. 8, it is seen that the strengthening of bridge piers using FRP increases a 12.8% of the bridge median fragility on average. The corresponding value for strengthening with a steel jacket, when models 3 vs. 6 and models 7 vs. 9 are compared, cause an average increase of 7.35% of the median fragility, indicating better performance of FRP as to steel jackets in reducing the probability of bridge vulnerability (Table 7).

The effects of abutment and foundation, the vertical component of the earthquake and strengthening of piers on the median fragility are estimated in Table 7, by comparing the different bridge models in the same conditions.

Table 7 The effects of abutment and foundation, the vertical component of the earthquake and strengthening of piers on the median fragility

	Slight	Moderate	Extensive	Complete	Average %
	Effect of Abutment and foundation				
Model 3 compared to 1	-9.289	-12.413	-15.642	-22.396	-14.935
Model 4 compared to 2	-16.101	-11.815	-1.919	-7.641	-9.369
				Total Average	-12.153
	Effect of vertical earthquake				
Model 3 compared to 7	-10.241	-9.055	-7.726	-6.862	-8.471
Model 5 compared to 8	-13.043	-12.195	-12.045	-9.923	-11.802
Model 6 compared to 9	-12.707	-11.870	-9.898	-11.748	-11.556
				Total Average	-10.609
	Effect of FRP in Retrofitting				
Model 5 compared to 3	10.843	12.992	15.452	20.404	14.923
Model 7 compared to 8	7.382	9.091	10.047	16.447	10.742
				Total Average	12.833
	Effect of Steel Jacketing in Retrofitting				
Model 3 compared to 6	9.036	9.448	9.271	9.007	9.191
Model 7 compared to 9	6.040	6.061	6.698	3.289	5.522
				Total Average	7.357

10. Bridge risk analysis

The hazard levels considered by FEMA 356 (2000) are:
(A) Hazard level -1: This level of risk is determined on the basis of a 10% probability of exceedance in 50 years, which is equivalent to 475-year mean return period (Eq. (13)).

$$\text{APE}^1 = 1 - \exp\left(-\frac{50}{475}\right) = 10\% \tag{13}$$

(B)   Hazard level -2: This level of risk is determined on the basis of a 2% probability of exceedance in 50 years, which is equivalent to 2475-year mean return period (Eq. (14)).

$$\text{APE} = 1 - \exp\left(-\frac{50}{2475}\right) = 2\% \tag{14}$$

These coefficients were attained by first obtaining a seismic hazard curve with respect to the existing faults for several points in each region, and then, by performing statistical calculations for each region, a coefficient is assigned to each of the hazard levels 1 and 2 in that area. To calculate the risk in the studied bridges at hazard levels 1 and 2, the risk analysis results performed by Abdolahzadeh *et al*. (2014) for northern Iran were implemented. These coefficients are shown in Figs. 20 and 21 for northern Iran.

As shown in Figs. 20 and 21, the peak ground acceleration (PGA) was between 0.3 to 0.35 at hazard level 1, and 0.65 to 0.7 at hazard level 2. The vulnerability of the examined bridges subjected to hazard levels 1 and 2 are respectively illustrated in Figs. 22 and 23.

---

[1]Annual Probability of Exceedance
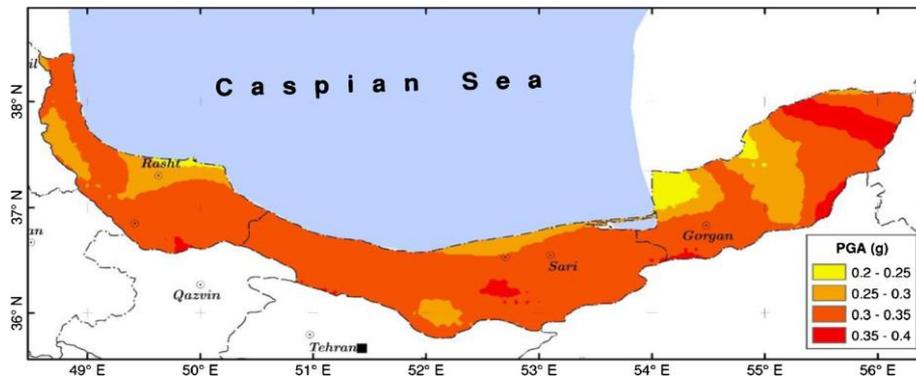
Fig. 20 Peak horizontal acceleration for the 475-year return period (Abdolahzadeh *et al.* 2014)
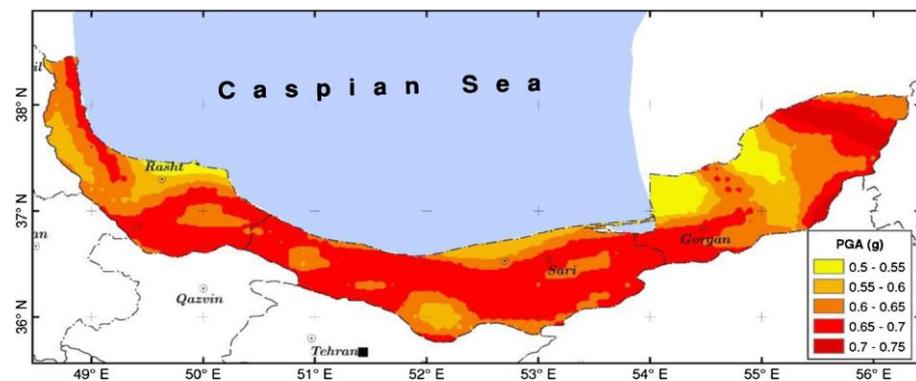
Fig. 21 Peak horizontal acceleration for the 2,475-year return period (Abdolahzadeh *et al*. 2014)

	Model 1	Model 2	Model 3	Model 4	Model 5	Model 6	Model 7	Model 8	Model 9
p (complete)	0.037	0.000	0.055	0.001	0.042	0.047	0.047	0.042	0.047
p (extensive)	0.335	0.037	0.394	0.062	0.345	0.360	0.367	0.345	0.360
p (Moderate)	0.586	0.086	0.650	0.147	0.591	0.609	0.619	0.591	0.609
p (slight)	0.774	0.234	0.817	0.334	0.772	0.785	0.795	0.772	0.785
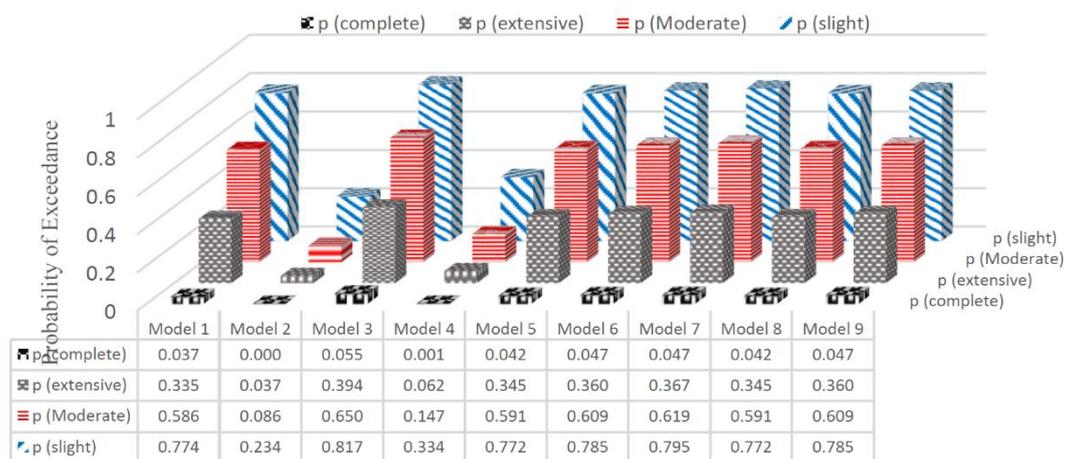
Fig. 22 Probability of vulnerability at hazard levels 1 (PGA=0.35 g)

As depicted in Figs. 22 and 23, the probability of vulnerability at hazard levels 1 and 2 has reduced sharply in models 2 and 4, which is owing to a 50% increase in the bridge columns diameter. This significantly reduces the probability of bridge failure.

	Model 1	Model 2	Model 3	Model 4	Model 5	Model 6	Model 7	Model 8	Model 9
p (complete)	0.137	0.006	0.189	0.010	0.153	0.170	0.151	0.153	0.170
p (extensive)	0.602	0.156	0.673	0.202	0.616	0.640	0.617	0.616	0.640
p (Moderate)	0.846	0.345	0.888	0.425	0.848	0.864	0.852	0.848	0.864
p (slight)	0.940	0.593	0.959	0.667	0.938	0.946	0.941	0.938	0.946
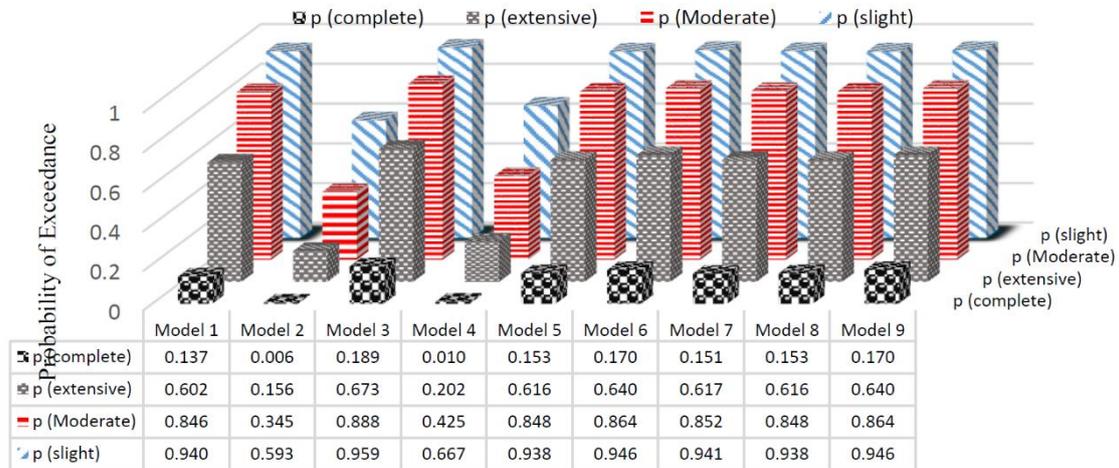
Fig. 23 Probability of vulnerability at hazard levels 2 (PGA=0.7 g)

11. Conclusions

Respecting the overall results, it is apparent to what extent a change in column diameter can affect the fragility curve. Comparing models 1 and 2 (models with column diameters of respectively 1 m and 1.5 m, and without the effects of abutment and foundation) demonstrates that in states of slight, moderate, extensive and complete damage, a 50% of increase in the column diameter multiplies the median fragility by a factor of 2.22, 2.21, 2.20 and 2.19, respectively. Such increase in models 3 and 4 (models with column diameters of respectively 1 m and 1.5 m that include the effects of abutment and foundation) are 1.99, 2.23, 2.72 and 3.47 times, respectively.

One of the common simplifications used in the modeling is to eliminate the effect of soil, abutment, foundation, and pile interaction, in which the vulnerability probability of the bridge is reduced and would thus be unrealistic. Generally, considering the effect of abutments and foundations in the model with a column diameter of 1 m (comparing models 1 and 3) in the four damage states of slight, moderate, extensive and complete decreases the median fragility by 9.3, 12.4, 15.6 and 22.4 %, respectively. For columns of 1.5 m diameter (comparing models 2 and 4), these values are respectively 16.1, 11.8, 1.9 and 7.6 %.

By comparing the results of model strengthened with FRP (model 5) with the initial unstrengthened model (model 3), it is perceived that the median fragility increased by 10.84, 12.9, 15.5 and 20.5 % respectively in the four damage states of slight, moderate, extensive and complete, expressing the (positive) effect of strengthening in this case. For the case of strengthening with steel jacket (model 6), the values (in percent) of median fragility increase were respectively 9.03, 9.4, 9.27 and 9, for the four damage states of slight, moderate, extensive and complete, which again confirms the effect of strengthening.

The median fragility is reduced by an average of 8.5%, 11.8%, and 11.55% respectively in the unstrengthened model with considering the vertical component of the earthquake, in the strengthened model with FRP, and in the strengthened model with a steel jacket. In general, considering the vertical component of the earthquake causes an average reduction of 6.10% in the median fragility and increases the vulnerability of the bridges in the course of an earthquake.

Acknowledgement

References

Abbasi, M., Zakeri, B. and Amiri, G.G. (2015), "Probabilistic seismic assessment of multiframe concrete box-girder bridges with unequal-height piers", *J. Perform. Constr. Facil.*, **30**(2), 04015016. https://doi.org/10.1061/(ASCE)CF.1943-5509.0000753.

Abdollahzadeh, G., Sazjini, M., Shahaky, M., Tajrishi, F.Z. and Khanmohammadi, L. (2014), "Considering potential seismic sources in earthquake hazard assessment for Northern Iran", *J. Seismol.*, **18**(3), 357-369. https://doi.org/10.1007/s10950-013-9412-1.

Alim, H. and Zisan, M.B. (2013), "Evaluation of probabilistic failure of bridge pire", *Int. J. Struct. Civil Eng.*, **2**(2), Research Paper, May.

Aviram, A., Mackie, K. and Stojadinovie, B. (2008), "Guidelines for nonlinear analysis bridge structure in Californai", Technical 2008/03, Pacific Earthquake Engineering Research Center, University of California, Berkeley.

Baker, J.W., Ling, T., Shahi, S.K. and Jayaram, N. (2011), "New ground motion selection procedures and selected motions for the PEER transportation research program", Draft Report, Pacific Earthquake Engineering Research Center, University of California, Berkeley.

Baloevic, G., Radnic, J., Grgic, N., Matesan, D. and Smilovic, M. (2016), "Numerical model for nonlinear analysis of composite concrete-steel-masonry bridges", *Coupl. Syst. Mech.*, **5**(1), 1-20. http://dx.doi.org/10.12989/csm.2016.5.1.001.

Bavirisetty, R., Vinayagamoorthy, M. and Duan, L. (2000), *Dynamic Analysis*, Bridge Engineering Handbook, Eds. W.F. Chen and L. Duan, CRC Press, Boca Raton, FL.

CALTRANS (2007), Reinforced Concrete Bridge Capacity Assessment Training Manual, Structure Maintenance and Investigations Rep., Sacramento, CA.

CALTRANS (2010-2012), Personal Communication with the P266 Fragility Project Advisory Panel Members Including Roblee,

Chang, G.A. and Mander, J.B. (1994), "Seismic energy based fatigue damage analysis of bridge columns, Part 1- Evaluation of seismic capacity", Technical Rep. NCEER-94-0006, State Univ. of New York, Buffalo, NY.

Choi, E. (2002), "Seismic analysis and retrofit of mid-America bridges", Ph.D. Thesis, Georgia Institute of Technology, Atlanta.

Dutta, A. (1999), "Energy based seismic analysis and design of highway bridges", Ph.D. Thesis, State Univ. of New York, Buffalo.

Ellingwood, B. and Hwang, H. (1985), "Probabilistic descriptions of resistance of safety related structures in nuclear plants", *Nucl. Eng. Des.*, **88**(2), 169-178. https://doi.org/10.1016/0029-5493(85)90059-7.

Falamarz-Sheikhabadi, M.R. and Zerva, A. (2017), "Analytical seismic assessment of a tall long-span curved reinforced-concrete bridge. Part I: numerical modeling and input excitation", *J. Earthq. Eng.*, **21**(8), 1305-1334. https://doi.org/10.1080/13632469.2016.1211565.

Fang, J., Li, Q., Jeary, A. and Liu, D. (1999), "Damping of tall buildings: Its evaluation and probabilistic characteristics", *Struct. Des. Tall Build.*, **8**(2), 145-153. https://doi.org/10.1002/(SICI)1099-1794(199906)8:2<145::AID-TAL127>3.0.CO;2-1.

FEMA356 (2000), Prestandard, Commentary for the Seismic Rehabilitation of Buildings, Washington, DC: Federal Emergency Management Agency, 7.

HAZUS-MH [Computer software], Federal Emergency Management Agency, Washington, DC.

Jeon, J.S., DesRoches, R., Kim, T. and Choi, E. (2016), "Geometric parameters affecting seismic fragilities of

curved multi-frame concrete box-girder bridges with integral abutments", *Eng. Struct.*, **122**, 121-143. https://doi.org/10.1016/j.engstruct.2016.04.037.

Jeon, J.S., Shafieezadeh, A., Lee, D.H., Choi, E. and DesRoches, R. (2015), "Damage assessment of older highway bridges subjected to three-dimensional ground motions: characterization of shear-axial force interaction on seismic fragilities", *Eng. Struct.*, **87**, 47-57. https://doi.org/10.1016/j.engstruct.2015.01.015.

Mandar, J.B., Priestley, M.J.N. and Park, R. (1988), "Observed stress strain behavior of confined concrete", *J. Struct. Eng.*, **114**(8), 1827-1849. https://doi.org/10.1061/(ASCE)0733-9445(1988)114:8(1827).

Mander, J.B., Kim, D.K., Chen, S.S. and Premus, G.J. (1996), "Response of steel bridge bearings to the reversed cyclic loading", Rep. No. NCEER 96-0014, NCEER.

McKenna, F., Scott, M.H. and Fenves, G.L. (2009), "Nonlinear finite-element analysis software architecture using object composition", *J. Comput. Civil Eng.*, **24**(1), 95-107. https://doi.org/10.1061/(ASCE)CP.1943-5487.0000002.

Megally, S.H., Silva, P.F. and Seible, F. (2001), "Seismic response of sacrificial shear keys in bridge abutments", Report No. SSRP-200l/23, Department of Structural Engineering, University of California, San Diego.

Menegotto, M. and Pinto, P.E. (1973), "Method of analysis for cyclically loaded reinforced concrete plane frames including changes in geometry and non-elastic behavior of elements under combined normal force and bending", *Proc., IABSE Symp. on Resistance and Ultimate Deformability of Structures Acted on by Well-Defined Repeated Loads*, Lisbon, Portugal.

Muthukumar, S. and DesRoches, R. (2006), "A Hertz contact model with non-linear damping for pounding simulation", *Earthq. Eng. Struct. Dyn.*, **35**(7), 811-828. https://doi.org/10.1002/eqe.557.

Naseri, A., Pahlavan, H. and Ghodrati Amiri, G. (2017), "Probabilistic seismic assessment of RC frame structures in North of Iran using fragility curves", *J. Struct. Constr. Eng.*, **4**(4), 58-78. https://doi.org/10.22065/jsce.2017.78827.1095.

Nielson, B. (2005), "Analytical fragility curves for highway bridges in moderate seismic zones", PhD Thesis, Georgia Institute of Technology.

OpenSEES [Computer software], Pacific Earthquake Engineering Research Center, Berkeley, CA.

Padgett, J.E. (2007), "Seismic vulnerability assessment of retrofitted bridges using probabilistic methods", Ph.D. Thesis, Georgia Institute of Technology, Atlanta.

Padgett, J.E. and DesRoches, R. (2008), "Methodology for the development of analytical fragility curves for retrofitted bridges", *Earthq. Eng. Struct. Dyn.*, **37**(8), 1157-1174. https://doi.org/10.1002/eqe.801.

Pahlavan, H. (2015), "Seismic fragility curve development for curved RC box-girder bridges", PhD Thesis, Iran University of Science and Technology, School of Civil Engineering.

Pahlavan, H., Naseri, A. and Einolahi, A. (2018), "Probabilistic seismic vulnerability assessment of RC frame structures retrofitted with steel jacketing", *Amirkabir Journal of Civil Engineering*. https://doi.org/10.22060/ceej.2018.13692.5459.

Pahlavan, H., Zakeri, B., Amiri, G.G. and Shaianfar, M. (2015), "Probabilistic vulnerability assessment of horizon-tally curved multiframe RC box-girder highway bridges", *J. Perform. Constr. Facil.*, **30**(3), 04015038. https://doi.org/10.1061/(ASCE)CF.1943-5509.0000780.

PEER, (Pacific Earthquake Engineering Research), Regents of the University of California, http://opensees.berkeley.edu/.

Raheem, S.E.A. (2018), "Structural control of cable-stayed bridges under traveling earthquake wave excitation", *Coupl. Syst. Mech.*, **7**(3), 269-280. http://dx.doi.org/10.12989/csm.2018.7.3.269.

Ramanathan, K., DesRoches, R. and Padgett, J.E. (2012), "A comparison of pre-and post-seismic design considerations in moderate seismic zones through the fragility assessment of multispan bridge classes", *Eng. Struct.*, **45**, 559-573. https://doi.org/10.1016/j.engstruct.2012.07.004.

Ramanathan, K.N. (2012), "Next generation seismic fragility curves for California bridges incorporating the evolution in seismic design philosophy", PhD Thesis, Georgia Institute of Technology, Atlanta.

Roshan, A.M.G., Naseri, A. and Pati, Y.M. (2018), "Probabilistic evaluation of seismic vulnerability of multi-span bridges in north of Iran", *J. Struct. Constr. Eng.*, **5**(1), 36-54. https://doi.org/10.22065/jsce.2017.68948.1009.

Saadeghvaziri, M.A. and Foutch, D.A. (1991), "Dynamic behavior of RC highway bridges under the combined effect vertical and horizontal earthquake motion", *Earthq. Eng. Struct. Dyn.*, **20**, 535-549. https://doi.org/10.1002/eqe.4290200604.

Sakino, K. (1994), "Stress-strain curve of concrete confined by rectilinear steels", *J. Struct. Constr. Eng.*, AIJ, **461**, 95-104.

Schrage, I. (1981), "Anchoring of Bearings by Friction", Joint Sealing and Bearing Systems for Concrete Structures, World Congress on Joints and Bearings, Vol. 1, Niagara Falls, NY, USA. American Concrete Inst.

Shamekhi amiri, M., Naseri, A. and Messgarpour amiri, M. (2019), "Seismic vulnerability assessment of reinforced concrete structures equipped with eccentrically braced frames having vertical link", *Amirkabir Journal of Civil Engineering*. https://doi.org/10.22060/ceej.2019.14313.5621.

Shamsabadi, A. and Yan, L. (2008), "Closed-form force-displacement backbone curves for bridge abutment backfill systems", *Proceedings of the Geotechnical Earthquake Engineering and Soil Dynamics IV Congress*, ASCE, 1-10. https://doi.org/10.1061/40975(318)159.

Shamsabadi, A., Khalili-Tehrani, P., Stewart, J.P. and Taciroglu, E. (2010), "Validated simulation models for lateral response of bridge abutments with typical backfills", *J. Bridge Eng.*, **15**(3), 302-311. https://doi.org/10.1061/(ASCE)BE.1943-5592.0000058.

Shaw, I.D. andrawes, B.O. (2017), "Finite element analysis of CFRP laminate repairs on damaged end regions of prestressed concrete bridge girders", *Adv. Comput. Des.*, **2**(2), 147-168. http://dx.doi.org/10.12989/acd.2017.2.2.147.

Shinozuka, M., Feng, M.Q., Kim, H.K. and Kim, S.H. (2000), "Nonlinear static procedure for fragility curve development", *J. Eng. Mech.*, **126**(12), 1287-1295. https://doi.org/10.1061/(ASCE)0733-9399(2000)126:12(1287).

Siqueira, G.H., Sanda, A.S., Paultre, P. and Padgett, J.E. (2014), "Fragility curves for isolated bridges in eastern Canada using experimental results", *Eng. Struct.*, **74**, 311-324. https://doi.org/10.1016/j.engstruct.2014.04.053.

Tondini N. and Stojadinovic. B. (2012), "Probabilistic seismic demand model for curved reinforced concrete bridges", *Bull. Earthq. Eng.*, **10**, 1455-1479. https://doi.org/10.1007/s10518-012-9362-y.

Wu, Y.F. and Wang, L.M. (2009), "Unified strength model for square and circular concrete columns confined by external jacket", *J. Struct. Eng.*, **135**(3), 253-261. https://doi.org/10.1061/(ASCE)0733-9445(2009)135:3(253).

Zhang, J. and Makris, N. (2002), "Seismic response analysis of highway overcrossings including soil structure interaction", *Earthq. Eng. Struct. Dyn.*, **31**(11), 1967-1991. https://doi.org/10.1002/eqe.197.

CC